

Fig. 3 Kinematic Reynolds shear stress bias (%) vs nondimensional distance from the wall (see text for legend definitions).

[by differentiating $\langle u \rangle(y_+)$ in the viscous sublayer⁸], Fig. 2 suggests that significant variations between the several correction methods would result. The determination of κ also utilizes much of the data set, through a statistical fit to Eq. (3), and again there appears to be little variation between the methods except, surprisingly, the GPC method, which predicts a value significantly lower than any other method. Compared with the commonly accepted value of $\kappa = 0.41$, this method is low by 6%. The intercept B in the logarithmic law is, of course, also obtained from a statistical fit of the data over most of the flow. Nevertheless, significant variability in the predicted value of B is seen between the several methods. Not surprisingly, the three inverse velocity correction methods yield very similar results, whereas straight arithmetic averaging, NC, predicts a value that is higher by 12%. The IA time and GPC methods yield values that are low by 7–9% compared with the inverse methods.

Conclusion

Although a statement of accuracy cannot be made without additional measurements, it is clear that relative deviations of $\pm 10\%$ can easily occur, depending on the bias correction scheme employed, when computing mean flow characteristics in similar wall-bounded flows. For some turbulence statistics, even larger deviations are possible.

Taken together with the other investigations cited in the references, it is concluded from this study that, in the case of low or intermediate data density, the proper choice of the bias correction method is vital if high-accuracy measurements, such as $\pm 2\%$, are required. Considering the literature on the experimental investigation of velocity bias for low or intermediate data densities, the selection of the appropriate method is not straightforward, and perhaps the best method may, unfortunately, be dependent on the flow that is under study.

References

- ¹Edwards, R. L., "Report of the Special Panel on Statistical Particle Bias Problems in Laser Anemometry," *Journal of Fluids Engineering*, Vol. 109, June 1987, pp. 89–93.
- ²McLaughlin, D. K., and Tiederman, W. G., "Biasing Correction for Individual Realization of Laser Anemometer Measurements in Turbulent Flows," *Physics of Fluids*, Vol. 16, No. 12, 1973, pp. 2082–2088.
- ³Nakao, S., Terao, Y., and Hirata, K., "New Method for Eliminating the Statistical Bias in Highly Turbulent Flow Measurements," *AIAA Journal*, Vol. 25, No. 3, 1987, pp. 443–447.
- ⁴Gould, R. D., and Loseke, K. W., "A Comparison of Four Velocity Bias Correction Techniques in Laser Doppler Velocimetry," *Journal of Fluids Engineering*, Vol. 115, Sept. 1993, pp. 508–514.

⁵Herrin, J. L., and Dutton, J. C., "An Investigation of LDV Velocity Bias Correction Techniques for High-Speed Separated Flows," *Experiments in Fluids*, Vol. 14, June 1993, pp. 354–363.

⁶Balakrishnan, M., and Dancy, C. L., "An Investigation of Turbulence in Open Channel Flow via Three-Component LDA," *Fundamentals and Advancements in Hydraulic Measurements and Experimentation, Proceedings of the Symposium*, American Society of Civil Engineers, New York, 1994, pp. 159–175.

⁷Dimotakis, P. E., "Single Scattering Particle Laser Doppler Measurements of Turbulence," AGARD CP-193, 1976.

⁸Durst, F., Kikura, H., Lekakis, I., Jovanovic, J., and Ye, Q., "Wall Shear Stress Determination from Near Wall Mean Velocity Data in Turbulent Pipe and Channel Flows," *Experiments in Fluids*, Vol. 19, July 1995, pp. 417–428.

G. Laufer
Associate Editor

Comparative Analysis of Deployable Truss Structures for Mesh Antenna Reflectors

Jin Mitsugi*
Nippon Telegraph and Telephone Corporation,
Yokosuka 239, Japan

I. Introduction

THE rapid growth of the Internet and information systems requires that high-capacity and ubiquitous communication be available for both voice and data transmission. Satellite communication, having the advantages of its inherent wireless access to the network, robustness against terrestrial disasters, and global coverage, is increasingly regarded as an essential element of the communication infrastructure. Accordingly, communication satellites are required to provide a number of spot beams covering their service areas to furnish high-capacity links for small, possibly portable, ground terminals. This task can be done by using a large deployable antenna on the satellite. A reflector antenna with an aperture of over 10 m will be needed to enable a satellite communication service with cellular-phone-size Earth terminals.¹ There are a number of structural concepts for large reflector antennas,² and of these, the combination of a deployable truss structure and a mesh reflector surface is considered reliable.³ Several deployable truss structure concepts have been presented, claiming large reflector antennas as one of their potential applications.

For the secure deployment of a mesh reflector, the deployment force of the truss structure must be larger than the deployment resisting force caused by the mesh surface, including an appropriate margin. As such, the design concept for a deployable truss structure should be evaluated in conjunction with the resisting mesh tension. It is, however, difficult to predict the resisting force of the mesh during deployment because it is a coupled problem that involves the mechanical motion of the truss structure and the elastic deformation of the mesh surface as well as the truss structure.

In this Note, two concepts of deployable truss structures are compared in view of the required deployment force against the mesh surface tension. The comparison was performed using the flexible multibody dynamics computer code that the author has developed.⁴ The formulation and the analytical procedure are not presented in this Note to focus on the comparison. This study does not intend to advocate that one deployable truss structure concept is better than the other but instead intends to unveil the essential differences in required deployment forces in accordance with the structural concepts.

Received July 12, 1997; revision received April 1, 1998; accepted for publication May 6, 1998. Copyright © 1998 by the American Institute of Aeronautics and Astronautics, Inc. All rights reserved.

*Senior Research Engineer, Wireless Systems Laboratory, Satellite Communication System Department, 1-1 Hikarino-oka. Member AIAA.

The two deployable truss structure concepts are introduced in Sec. II. The comparative analysis on the truss structures is presented in Sec. III.

II. Computational Models

There are two types of deployable truss structures, both of which are hexagonally shaped hoops in the deployed configuration (Fig. 1). In one concept, referred to as a slide-type truss structure, a sliding mechanism is the prime deployment mechanism (Fig. 1). This type of truss structure, excluding articulated members, has been proposed by Watanabe et al.⁵ and Onoda et al.⁶

In the other concept, referred to as an articulated-type truss structure, a side is composed of two articulated truss members and a scissor-shaped link that synchronizes the deployment motion and braces the truss structure (Fig. 2). Examples of this type of truss structure, using articulated truss members as the primal deployment mechanism, are the Japanese Advanced Space Communications Research Laboratory (ASC) reflector⁷ and the Aerospatiale reflector.⁸ The deployment motion of the articulated type was computationally modeled by simultaneously extending or shortening the terminal points of the six articulated members.

The depth of both truss structures in the computation was 600 mm, and the length of the top hexagon sides in the deployed state was 500 mm. These dimensions represented a basic structure for the deployable reflector presented in Ref. 5. Outer and inner diameters of the truss member are 18 and 16 mm, respectively.

An identical mesh surface model, represented by a cable network, was connected to each of the two truss structures. The cable network

was composed of 61 cables located in both the radial and tangential directions (Fig. 3).

III. Comparison

Cable tension profiles were computed using transient dynamic analysis in accordance with the deployment motion. The deployment motion was represented by deployment angle. The deployed and stowed configurations of both truss structures were represented by deployment angles of 0.0 and $\pi/2$ rad, respectively (Fig. 4). Cable tensions of the slide type gradually decrease as the truss structure is stowed (Fig. 5). Because the truss members were positioned only in a hoop manner, tensions in the radial cables decreased faster than those of the tangent cables. The cable tensions in the articulated-type truss are shown in Fig. 6. All of the cables lost tension at approximately

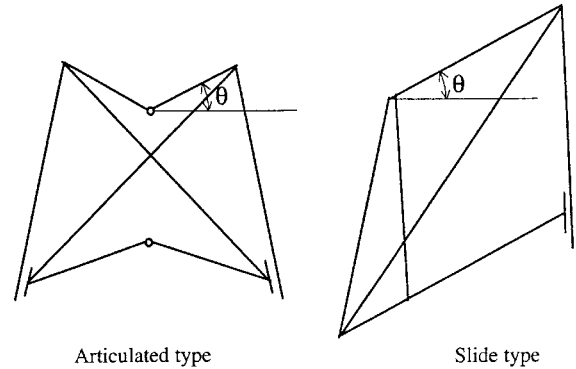


Fig. 4 Deployment angle definition.

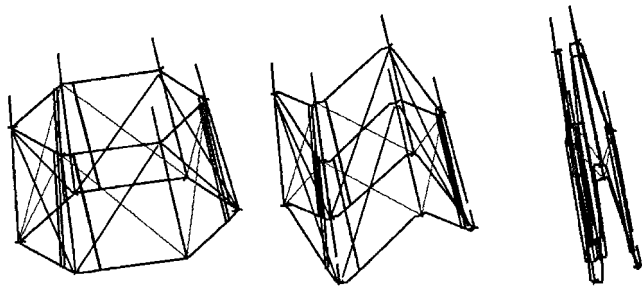


Fig. 1 Deployment motion of slide-type truss structure.

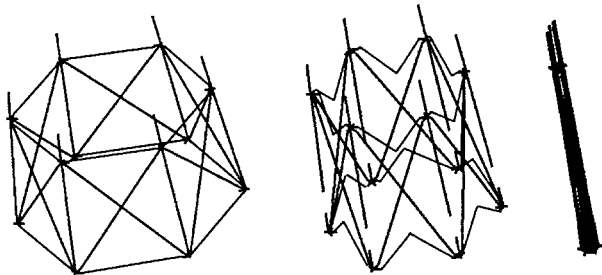


Fig. 2 Typical deployment motion of articulated-type truss structure.

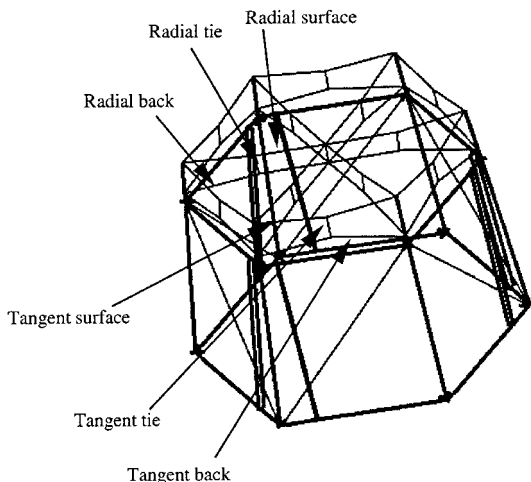


Fig. 3 Cable network model.

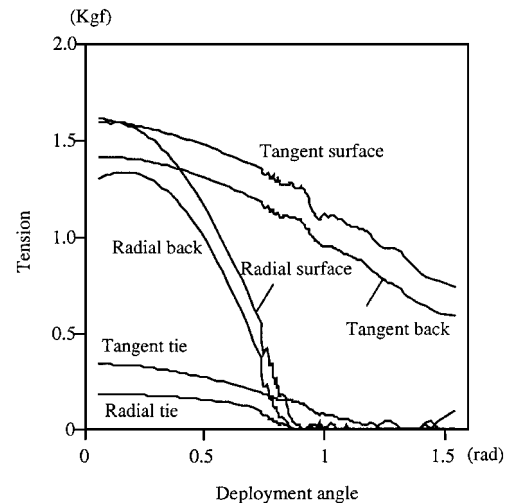


Fig. 5 Cable tension profile of slide-type truss.

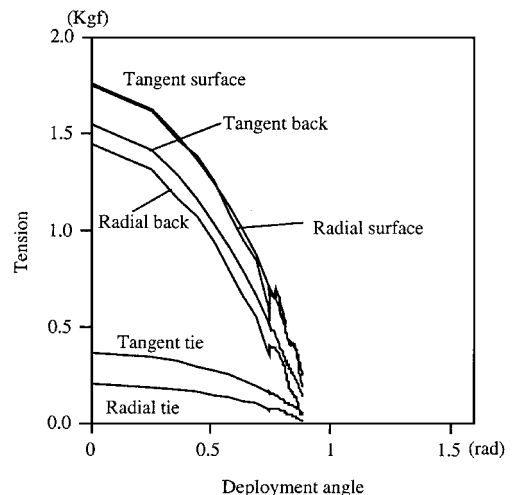


Fig. 6 Tension profile of the articulated-type truss.

0.9 rad. No major discrepancy was observed between the radial and tangent cable tension. In an articulated type, therefore, the deployment driving force is required only from 0.0 to 0.9 rad in terms of deployment angle because all of the cables lose tension between 0.9 and 1.5 rad. Because the same amount of energy should be stored in the mesh surface regardless the type of truss structure, the short drive stroke entails large peak deployment force. Consequently, the peak deployment driving force of an articulated type is larger than that of a slide type when deploying an identical mesh surface.

IV. Conclusion

In summary, an articulated type requires a larger peak force and shorter stroke deployment mechanism than a slide-type truss structure. The choice of the truss structure, however, depends on the designated force margin and weight restriction.

References

- ¹Samejima, S., "Roles of Geostationary and Non-Geostationary Satellites for Mobile Communications," *MWE '95 Microwave Digest*, 1995, pp. 281–286.
- ²Naderi, F., "Large Space-Borne Antenna Technology: A System Perspective," NASA CP-2269, Pt. 1, Dec. 1982, pp. 1–16.

³Rogers, C. A., Stuzman, W. L., Campbell, T. G., and Hedgepeth, J. M., "Technology Assessment and Development of Large Deployable Antennas," *Journal of Aerospace Engineering*, Vol. 6, No. 1, 1993, pp. 34–54.

⁴Mitsugi, J., "Direct Coordinate Partitioning for Multibody Dynamics Based on Finite Element Method," *Proceedings of the 36th Structures, Structural Dynamics, and Materials Conference*, AIAA, Washington, DC, 1995, pp. 2481–2487 (AIAA Paper 95-1442).

⁵Watanabe, M., Meguro, A., Mitsugi, J., and Tsunoda, H., "Module Composition and Deployment Method on Deployable Modular-Mesh Antenna Structures," *Acta Astronautica*, Vol. 39, No. 7, 1996, pp. 497–505.

⁶Onoda, J., Fu, D. Y., and Minesugi, K., "Two-Dimensionally Deployable Hexapod Truss," AIAA 95-1279, 1995.

⁷Horiuchi, Y., Inoue, M., Miyoshi, K., Sugimoto, T., Okamoto, T., and Hariu, K., "Development of Magnetically Suspended Sliders for Deployable Antenna Test Facility," 5th International Symposium on Magnetic Bearings, 5B, Japan Society of Mechanical Engineers, Aug. 1996.

⁸Flechaix, A., Picard, P., Dauviau, C., and Truchi, C., "Dynamics of Large Reflectors AEROSPATIALE Concepts," 43rd Congress of the International Astronautical Federation, IAF Paper 92-0307, Washington, DC, Sept. 1992.

A. D. Belegundu
Associate Editor